



ARTICLE

Coupled Effects of Heat and Moisture of Early-Age Concrete

Yang Wang¹, Hanxi Wang^{2,*}, Linwei Yang¹ and Li Qian¹

¹School of Urban Construction and Transportation, Hefei University, Hefei, 230601, China

²School of Electronic Science and Applied Physics, Hefei University of Technology, Hefei, 230601, China

*Corresponding Author: Hanxi Wang. Email: 2020213561@mail.hfut.edu.cn

Received: 26 January 2021 Accepted: 26 March 2021

ABSTRACT

In order to analyze the coupled influence of temperature and humidity on early-age concrete (including cement and copper tailings), a mathematical model is introduced on the basis of the Krstulovic-Dabic hydration reaction kinetic equations. In such a framework, the influence of hydration-released heat and water consumption are also taken into account. The results provided by such a model are verified by means of experiments and related sensor measurements. The research results show that this model can adequately predict the internal temperature and the humidity temporal evolution laws.

KEYWORDS

Composite cementitious materials; cement hydration; micro-structure; diffusion coefficient; coupled of heat and moisture

Nomenclature

A :	empirical coefficient, m/h
a :	constant related to temperature
B :	empirical coefficient, m/h
b :	constant related to humidity
C :	specific heat capacity of concrete, J/(kg·°C)
D :	hydration degree, %
D_c :	hydration degree of cement, %
D_{28} :	hydration degree when cement is hydrated for 28 days, %
E :	activation energy of hydration, J/mol
E_s :	diffusion activation energy, J/mol
F_w :	humidity flux
H :	hydration relative humidity, %
H_s :	relative humidity induced by self-drying of concrete, %
H_{s-max} :	maximum relative humidity induced by self-drying of concrete, %
H_E :	relative humidity of surrounding environment, %
h :	constant related to porosity
K_{NG} :	rate constant of NG process
K_I :	rate constant of I process
K_D :	rate constant of D process



K_H :	material parameter related to humidity diffusion, concrete pore structure, and temperature
K_M :	material parameter depending on the water-binder ratio
m_c :	mass of cement, kg
m_t :	mass of copper tailings, kg
n :	constant related to mineral composition
P :	copper tailings mixing ratio, %
Q :	heat release during hydration, J
Q_T :	total heat release of cement, J
Q_i :	total heat release of cement and copper tailings, J
Q_{c-max} :	maximum heat release of cement, J
Q_{t-max} :	maximum heat release of copper tailings, J
R_0 :	initial radius of cement particle, m
R^* :	gas constant
S :	moisture diffusion coefficient of concrete
S_0 :	diffusion coefficient of concrete under water saturation at T_0 , m^2/h
T :	hydration temperature, $^{\circ}C$
T_E :	ambient temperature, $^{\circ}C$
T_0 :	standard temperature, $20^{\circ}C$
t :	reaction time, h
t_0 :	initial time of hydration, h
t_h :	time when hydration heat reaches the half of total heat, h
W_v :	volumetric moisture content, m^3/m^3
$\alpha_1 \sim \alpha_6$:	reduction coefficients for change rate of cement particle radius
α :	total porosity of cement paste mixed with copper tailings, %
α_{28} :	porosity of concrete at 28 days of age, %
α_c :	porosity of cement, %
α_t :	porosity of copper tailings, %
$\beta_1 \sim \beta_3$:	influence coefficients for change rate of copper tailings particle radius
β_T :	exothermic coefficient of concrete surface, $J/(h \cdot m^2 \cdot ^{\circ}C)$
γ :	humidity exchange coefficient
ρ :	concrete density, kg/m^3
λ :	thermal conductivity of concrete, $J/(h \cdot m \cdot ^{\circ}C)$
η_1, η_2 :	adjustment coefficients of hydration reaction rate
ΔD_S :	increment of cement hydration degree, %
ΔD_P :	increment of copper tailings hydration degree, %
w/b :	water-binder ratio

1 Introduction

Due to huge production of concrete, it is necessary to use mineral admixtures with abundant sources and low cost in practical applications. Copper tailings are waste residues discharged after the extraction of useful metals such as copper and gold. It is a typical industrial waste with large amount and small particle size.

Many researchers had been concerned the coupling effects of heat and moisture diffusion of early-age concrete. Based on cement hydration kinetics model, the coupled diffusion characteristics of temperature and humidity was studied [1,2], while the coupling mechanism of concrete at early age was not clarified yet. Based on the Weibull distribution theory, the moisture-heat chemical model from the perspective of micromechanics had been established [3], which took the coupling of dampness, heat and hydration into

account. The diffusion equation of Fick's second law was applied in simulating the relative humidity field of concrete [4], but the factor of water consumption due to self-drying was ignored. The finite difference method was used to simulate the relative humidity field of concrete [5], and self-drying and diffusion processes were considered, but the coupling effect of temperature and relative humidity was not considered.

Krstulovic et al. [6] proposed a dynamic model for hydration reaction of cement-based materials, in which hydration reaction was divided into three basic processes: crystallization nucleation and crystal growth (NG), interactions at phase boundaries (I), and diffusion process (D).

The present kinetics studies on the basis of the Krstulovic-Dabic model are mostly focused on conventional cement mixtures such as fly ash, slag and silica fume. The model was employed to study hydration heat release law of mass concrete [7], and it had been found that cement mixed with a certain amount of mineral admixtures had longer acceleration and deceleration periods. The influence on hydration kinetic parameters was discussed, and the change of hydration process after adding the admixture was analyzed [8]. The hydration process of C_3S was investigated [9], in which it was found that the addition of fly ash was unable to change the type of hydration process.

However, cement active admixtures such as fly ash are becoming increasingly scarce. In view of low cost of industrial waste and production of "green cement", in this paper, we focus on how to make full use of copper tailings as cement admixtures or concrete composite materials, which can provide a theoretical guidance for large-scale utilization of various solid industrial wastes such as quartz tailings, iron tailings, steel slag, etc.

This paper proposes an improved hydration model of mineral admixtures incorporating the effect of copper tailings on the hydration process of cement. The hydration degree, hydration rate and porosity are obtained. Related parameters are further introduced into the concrete temperature and humidity diffusion equation. The coupling model of heat and moisture for early-age concrete is created and is verified by subsequent test data.

2 Cement-Copper Tailings Hydration Kinetics

2.1 Hydration Model of Portland Cement

According to Krstulovic-Dabic model, the kinetic equations and their corresponding differential equations between hydration degree (D) and reaction time (t) are given as below (the diffusion process is calculated by the Jander reaction model [10]),

NG process:

$$K_{NG}(t - t_0) = [-\ln(1 - D)]^{\frac{1}{n}} \quad (1)$$

$$\frac{dD}{dt} = K_{NG}n(1 - D)[- \ln(1 - D)]^{1-\frac{1}{n}} \quad (2)$$

I process:

$$K_I(t - t_0) = 1 - (1 - D)^{\frac{1}{3}} \quad (3)$$

$$\frac{dD}{dt} = 3K_I(1 - D)^{\frac{2}{3}} \quad (4)$$

D process:

$$K_D(t - t_0) = \left[1 - (1 - D)^{\frac{1}{3}}\right]^2 \quad (5)$$

$$\frac{dD}{dt} = \frac{3}{2} K_D (1-D)^{\frac{2}{3}} \left[1 - (1-D)^{\frac{1}{3}} \right]^{-1} \quad (6)$$

in which K_{NG} , K_I , and K_D are rate constants for the three processes, respectively, n is a constant related to cement mineral composition, and t_0 is the initial time of hydration after the end of cement induction period.

Cement hydration is mainly related to some factors such as concrete components, water-binder ratio, moisture content, environmental temperature and humidity, etc. The heat release during hydration process (Q) can be expressed as a function of hydration degree [11],

$$Q = D \cdot Q_T \quad (7)$$

where D is hydration degree, Q_T is the total heat release after the cement is completely hydrated.

The total heat release of Portland cement can be determined by the Knudsen extrapolation equation [12]. The relationship between heat release (Q) and cement hydration time (t) is written as below:

$$Q = \frac{Q_T(t - t_0)}{t + t_h - t_0} \quad (8)$$

in which t_h is the time when heat release reaches the half of total heat release.

Cement hydration degree can be denoted as the ratio of heat release to the total heat release. It is assumed that copper tailings are uniformly distributed, and the heat release is proportional to the volume of the particle. Then the hydration degree of the cement particle with an initial radius R_0 can be indicated as,

$$D = \frac{Q}{Q_T} = 1 - \frac{R(t)^3}{R_0^3} \quad (9)$$

where Q is the heat release of cement particles after being hydrated for time t ; $R(t)$ is the radius of cement particle with initial radius of R_0 at time t .

Substituting Eq. (9) into the Krstulovic-Dabic equations can attain the variation of cement particle radius per unit time of hydration:

$$dR_{NG} = \frac{1}{3} n K_{NG} R(t) [-3 \ln(R(t)/R_0)]^{\frac{1}{n}} dt \quad (10)$$

$$dR_I = K_I R_0 dt \quad (11)$$

$$dR_D = \frac{1}{2} K_D R_0^2 [R_0 - R(t)]^{-1} dt \quad (12)$$

in which dR_{NG} , dR_I , dR_D are the radius reduction of cement particles with initial radius of R_0 in the three processes of hydration, respectively.

According to the principle of Minimum Energy Consumption, the theoretical change rate of cement hydration particle radius (dR) takes the minimum value,

$$dR = \min[dR_1, dR_2, dR_3] \quad (13)$$

In this way, the relations among hydration heat release, hydration reaction time, hydration degree and cement particle size are set up.

2.2 Hydration Model of Cement Mixed with Copper Tailings

The hydration of composite cementitious materials consists of cement hydration and copper tailings hydration. X-ray diffraction analysis confirmed that copper tailings particles have the same microscopic

hydration unit as cement particles [13], so the hydration kinetics process can be controlled by the three equations of Krstulovic-Dabic model.

The hydration degree of copper tailings can also be calculated by Eqs. (7)–(13), but the reaction constants K_{NG} , K_f , K_D , n are different from those of cement. Adding copper tailings may affect cement hydration process including dilution effect, physical effect and chemical impact [13,14].

The final hydration degree of cement-based material is proportional to its effective water-cement ratio. When the proportion of copper tailings increases, the effective water-cement ratio also grows, and thus the hydration process of the composite cementitious system is delayed. This phenomenon is called dilution effect.

Copper tailings as an admixture can improve filling effect and lubrication effect of cement-based material. It exerts two physical effects on cement hydration: delaying the hydration in the early stage; increasing hydration degree of the cement particle in hydration process.

The chemical impact of copper tailings is mainly manifested as follows: copper tailings contain lots of active substances; during the hydration, cement and copper tailings need water to complete the reaction; if the dosage of copper tailings is too large, there will be a peak value in water consumption, which hinders cement hydration.

Considering the impact of copper tailings, the cement hydration degree (D_c) is represented as,

$$D_c = (1 + \Delta D_S)(1 + \Delta D_P)D \quad (14)$$

where ΔD_S is the increment of cement hydration degree caused by the dilution effect of copper tailings, ΔD_P is the increment induced by the physical acceleration effect of copper tailings.

In hydration process of composite cementitious materials, water reduction, pore saturation, temperature, contacting area between cement and water, copper tailings and other factors all affect the rate of change of cement particle radius. The modified change rate of cement particle radius is,

$$dR_c(D_c) = \alpha_1 \alpha_2 \alpha_3 \alpha_4 \alpha_5 \alpha_6 D_c dR \quad (15)$$

in which α_1 is relevant to the water content of hydration unit, α_2 concerned with pore saturation, α_3 related to temperature, α_4 involved with the change of hydration degree, α_5 the reduction coefficient of variation of cement particle radius, α_6 the retardation effect coefficient of copper tailings on cement hydration [10,14].

Likewise, considering the impact of water consumption and the reduction of the contact area between particles and water, the final change rate of the copper tailings particle radius can be presented as,

$$dR_t(D_t) = \beta_1 \beta_2 \beta_3 dR' \quad (16)$$

where β_1 is the influence coefficient due to the decrease of water content, β_2 the coefficient concerned with contact area between copper tailings and water, β_3 the temperature parameter affecting particle radius, dR' the minimum change rate of particle radius.

3 Coupled Model of Heat and Moisture

3.1 Model Controlled by Temperature Field

In this paper, the hydration microscopic model is connected with the temperature field of concrete by means of the hydration reaction rate. Taking the change of temperature and humidity, hydration degree and hydration age into account [10], the temperature control equations are written as,

$$\rho C \frac{\partial T}{\partial t} = \nabla \cdot (\lambda \nabla T) + f(T, H) \sum Q_i \frac{\partial D_i}{\partial t} \quad (17)$$

$$f(T, H) = [1 + (\eta_1 - \eta_1 H)^{\eta_2}]^{-1} e^{-\frac{E}{R^*(T+273.15)}} \quad (18)$$

in which T is the temperature, H the relative humidity, ρ the concrete density, C the specific heat capacity of concrete, λ the thermal conductivity of concrete, $f(T, H)$ the influence coefficient of temperature and relative humidity on the hydration reaction rate [15], E the activation energy of hydration, R^* the gas constant, Q_i the total heat release of cement and copper tailings, η_1 and η_2 the adjustment coefficients.

$$Q_i = Q_c + Q_t = m_c Q_{c-\max} + m_t Q_{t-\max} \quad (19)$$

in which m_c is the mass of cement, m_t the mass of copper tailings, $Q_{c-\max}$ the maximum heat release of cement, and $Q_{t-\max}$ the maximum heat release of copper tailings.

The boundary condition is presented,

$$-(\lambda \nabla T) = \beta_T (T - T_E) \quad (20)$$

where β_T is the exothermic coefficient of concrete surface, and T_E the ambient temperature.

3.2 Moisture Diffusion Model

Here, the humidity characteristics of concrete is described by the relative humidity of concrete. The relation between volumetric moisture content (W_v) and humidity flux (F_w) can be given as follows [16,17]:

$$\frac{\partial W_v}{\partial t} = \frac{\partial W_v}{\partial H} \frac{\partial H}{\partial t} = \nabla \cdot (K_H \nabla H) = -\nabla F_w \quad (21)$$

in which K_H is a parameter related to humidity diffusion, concrete pore structure, and temperature. For simplicity, neglecting the self-drying effect caused by the hydration of copper tailings, the nonlinear relative humidity diffusion equation is presented,

$$\frac{\partial H}{\partial t} = \nabla \cdot \left(K_H \frac{\partial W_v}{\partial H} \nabla H \right) + \frac{\partial H_s}{\partial t} = \nabla \cdot (S \nabla H) + \frac{\partial H_s}{\partial t} \quad (22)$$

where S is the moisture diffusion coefficient of concrete, H_s the relative humidity induced by self-drying of concrete only. Thereby, the influence coefficient on the hydration rate $f(T, H)$ is utilized to reflect the effect of changes on self-drying effect, and the coupling relation of temperature and humidity can be established as,

$$\frac{\partial H_s}{\partial t} = \frac{\partial H_s}{\partial D} \frac{\partial D}{\partial t} = (H_{s-\max} - 1) \frac{K_M}{D_{28}} \left(\frac{D}{D_{28}} \right)^{K_M-1} f(T, H) \quad (23)$$

where D_{28} is the hydration degree when cement is hydrated for 28 days, $H_{s-\max}$ maximum relative humidity induced by self-drying of concrete, which can be obtained by inverse deduction from Isothermal Adsorption model [18], and K_M the material parameter depending on the water-binder ratio.

The boundary condition is provided as follows:

$$-(S \nabla H) = \gamma (H - H_E) \quad (24)$$

where H_E is the relative humidity of surrounding environment, γ the humidity exchange coefficient on the surface of the concrete, which represents the diffusion characteristics of moisture in the air. Here, the

expression proposed in reference [19] is used: $\gamma = A(w/b)-B$, in which w/b is the water-binder ratio, A and B are the empirical coefficients, respectively.

3.3 Modification of Diffusion Coefficient Considering Coupled Effect

Apart from the influence of relative humidity and temperature on the humidity diffusion coefficient [16], the evolution of the microstructure at the early age will also affect the humidity diffusion. The effects of age and porosity were both taken into account for humidity diffusion coefficient [20]. In summary, the humidity diffusion coefficient involving the influence of porosity is listed as,

$$S(H, T, \alpha) = S_0 f_1(H) f_2(T) f_3(\alpha) \quad (25)$$

$$f_1(H) = \frac{1}{T_0} + \frac{(T_0 - 1)/T_0}{1 + [(1 - H)/(1 - a)]^b} \quad (26)$$

$$f_2(T) = \left(\frac{T_0 + 273.15}{T + 273.15} \right)^{1.5} \exp \left[\frac{E_s}{R} \left(\frac{1}{T_0 + 273.15} - \frac{1}{T + 273.15} \right) \right] \quad (27)$$

$$f_3(\alpha) = \left(\frac{\alpha}{\alpha_{28}} \right)^h = \left[\frac{\alpha_c(1 - P) + \alpha_t P}{\alpha_{28}} \right]^h \quad (28)$$

where T_0 is the standard temperature (20°C), S_0 the diffusion coefficient of concrete under water saturation at T_0 , α_{28} the concrete porosity at 28 days of hydration age, E_s the diffusion activation energy, and P the copper tailings mixing ratio. a , b , h are constants, respectively. α_c , α_t are the porosities of cement and copper tailings, respectively, which can be obtained by particle size distribution function (see reference [21]).

α is the total porosity of cement paste mixed with copper tailings, which can be obtained by Eq. (29),

$$\alpha = \alpha_c(1 - P) + \alpha_t P \quad (29)$$

4 Comparison of Values between Calculation and Experiment

4.1 Experimental Overview

After the selected copper tailings are filtered by pressure, they are calcined in a rotary kiln at 1300–1500°C for 1.5–3 min, then ground into copper tailings powder with a specific surface area of 476–512 m²/kg, whose chemical composition is shown in Tab. 1 (chemical titration analysis results). The corresponding mineral composition is shown in Tab. 2 (XRF analysis results). With a water-binder ratio 0.40, the selected cement is Portland cement of grade 42.5, the proportion of copper tailings is 30%, and the mixing proportion of concrete is the following: *cement: water: sand: stone: copper tailings* = 0.70: 0.40: 1.61: 2.53: 0.30.

Table 1: Main chemical composition of copper tailings for experiment (wt%)

Composition	SiO ₂	CaO	MgO	Al ₂ O ₃	Fe ₂ O ₃	TiO ₂	Loss
Percentage	42.19	27.58	2.32	6.78	8.53	0.08	11.67

Table 2: Mineral composition of copper tailings (wt%)

Mineral name	Calcite	Andradite	Wollastonite	Quartz
Chemical formula	CaCO ₃	Ca ₃ Fe ₂ [SiO ₄] ₃	Ca ₃ [Si ₅ O ₉]	SiO ₂
Percentage	10–20	20–40	15–30	5–15

Some wooden thermal insulation molds lined with plastic film have been prepared with the size $400 \times 250 \times 250$ mm. Concrete with specified mix proportion is poured in the molds (Fig. 1a) and the thermocouple sensors (Ahlborn NiCr-Ni and FHA6x6) are directly embedded from the upper open side with embedded depths 180, 100, 30 mm, respectively (Fig. 1b). The front end of each temperature sensor is wrapped with plasticine, and the front end of the moisture sensor is wrapped with permeable and breathable fiber woven fabric and covered with porous protective tube. These sensors have high precision without data drift after long-term measurement. The back end is connected with Ahlborn MU-56901 desktop data acquisition instrument (Fig. 1c), which collects and stores data regularly and automatically [22].

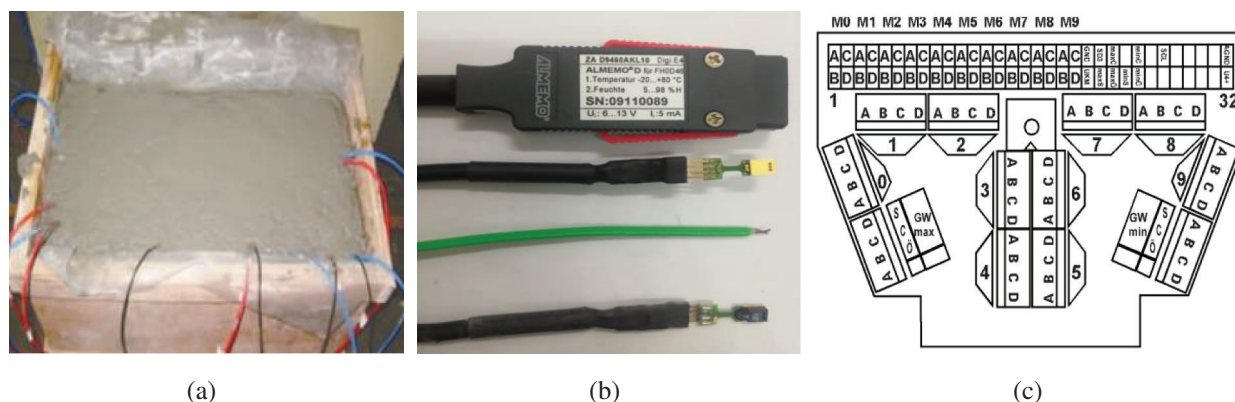


Figure 1: Part of experimental devices. (a) Concrete sample. (b) Front end of temperature and humidity sensors. (c) Ahlborn MU-56901 multi-channel interfaces

According to the information of raw materials (chemical composition, particle size distribution of cement and copper tailings, water-binder ratio), one can derive the hydration degree (D), the hydration rate (dD/dt) and the particle radius change rate (dR/dt), and further temperature field (T) and humidity field (H). The hydration process can be predicted by determining whether the set time is reached through cyclic calculation.

Software FLAC3D5.0 and MATLAB-R2015a are selected to solve the nonlinear equations in the temperature and humidity coupling 1-D model [23], which can provide interactive operation interfaces. In order to simplify the calculation and set the critical value, the following steps in modeling are presented,

- (1) Analysis module, select coefficient module to calculate Eqs. (17), (21–23).
- (2) Geometric modeling, the upper surface of the concrete test block is treated as the boundary layer, then the mesh is divided, the model size is $400 \times 250 \times 250$ mm, the time step is set to 0.5 h, there are 48050 grid cells and 52224 nodes (Fig. 2).
- (3) Parameter setting, when the strength grade of concrete is C50, the typical values of constants, parameters and coefficients are shown in Tabs. 3–5.
- (4) Boundary conditions, use Cauchy boundary conditions Eqs. (20) and (24).

4.2 Parameters Verification

The comparison between calculated values of the microscopic hydration model and experimental hydration values is shown in Fig. 3. The calculated results are in good agreement with the measured values. In the early stage of hydration, the calculated values are generally slightly larger than those of experiments and the error is relatively large when water-binder ratio is 0.54, which is because water

content in the hydration model is sensitive to the change of the radius of cement particles. When water content is large, the hydration rate is faster and the error becomes larger. In the late period of hydration (after 7 days), the error of hydration degree with different water-binder ratios is smaller, which can demonstrate that the microscopic hydration model proposed is accurate.

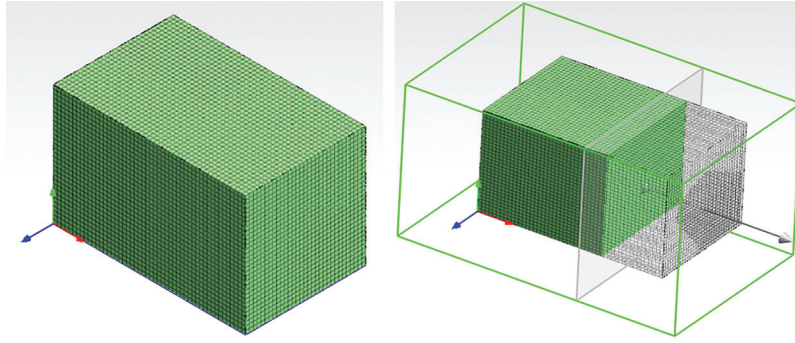


Figure 2: 3D view of concrete test block and cut surface

Table 3: Hydration kinetics parameters [10,14]

Cementitious materials	n	K_{NG}	K_I	K_D
Cement	1.54	0.0612	0.022	0.005
Copper tailings	1.08	0.000156	0.000132	0.0018

Table 4: Parameters for heat and moisture coupling (R-SI) [9,10,13,14,24]

Parameters	β_T	ρ	C	λ_0	S_0	A	B	E_S/R	E/R
Unit	J/(h·m ² ·°C)	kg/m ³	J/(kg·°C)	J/(h·m·°C)	m ² /h	m/h	m/h	K	K
Value	80000	2390	1007.5	8948.3	2.10×10^{-6}	2.232×10^{-3}	0.9×10^{-3}	2700	5000

Table 5: Coefficient values in the equations [9,10,13,24]

Coefficient	w/b	η_1	η_2	h	a	b	H_{s-max}	K_M
Value	0.45	5.5	4	0.75	4	3	0.88	4

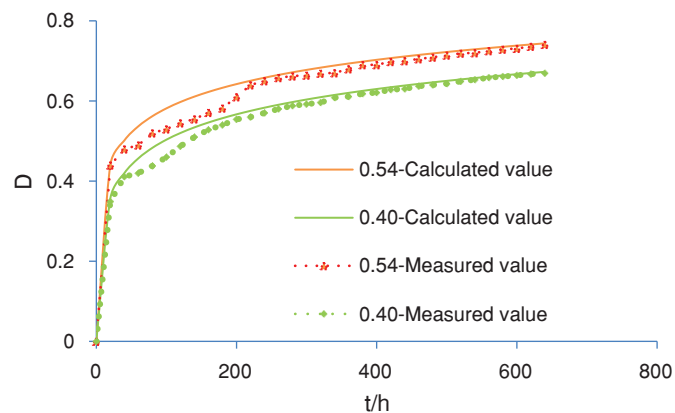


Figure 3: Comparison between calculated and measured values of hydration degree

The content of copper tailings is set to 30%, and the water-binder ratio is set to 0.4 in making C50 concrete. The comparison between calculated and measured values of temperature within 7 days is provided in Fig. 4. It can be seen that due to the exothermic effect of hydration at the initial stage, the temperature rises in a short period of time and forms a high temperature gradient, which is roughly eliminated after 90 hours. When the sensor is embedded at a depth of 30 mm, the deviation between calculated and measured values is large. That is because the measuring point is close to the surface of concrete and is greatly affected by ambient temperature, measurement error and heat dissipation.

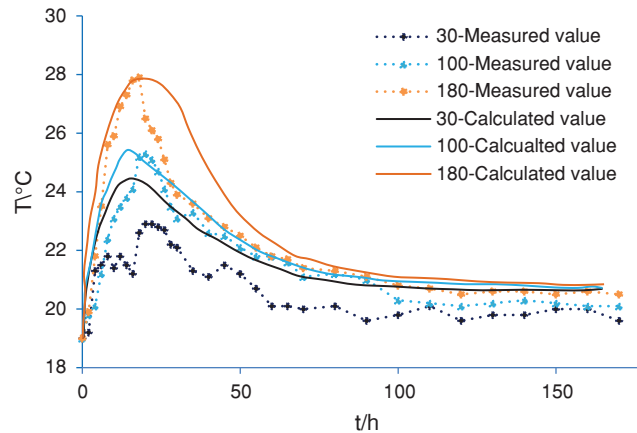


Figure 4: Comparison between calculated and measured values of temperature

The calculated and measured values of relative humidity within 28 days of each measuring point are presented in Fig. 5. Generally speaking, as the depth of the test point increases, the relative humidity of concrete rises. In accordance with the theory of free water migration, free water migrates to the direction of low humidity [25]. Since the humidity of surrounding environment is smaller than that in the interior of the concrete, free water will migrate from the inside of the concrete to the outside environment at the initial stage of setting and hardening.

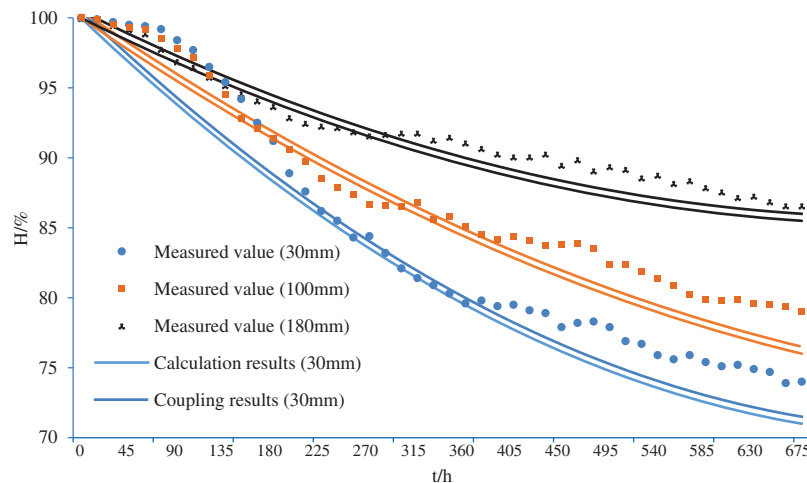


Figure 5: Comparison of calculation and experimental values of humidity

In the early stage of hydration, the calculation values and measured values are quite different, the latter is significantly large. This may be due to that the temperature and the humidity are relatively high in the early stage of hydration, so that water accumulation happens in the sensors, thereby resulting in large measurement errors.

Basically, the measured and calculated results are in good agreement, especially in the middle and late stages.

In order to explore the influences of different copper tailings content on hydration process, cementitious material pastes were prepared to observe the hydration products [26]. It can be seen from the SEM photo (Fig. 6) that pure cement paste has formed a continuous cross-linked network structure in the early stage. Adding a certain amount of copper tailings can generate more abundant hydration products, when the amount of copper tailings is large, the structural compactness and C-S-H gel are reduced and more non-gel substances appear in the hydration product, which has negative effect on hydration to a certain extent, in the meantime, the cement slurry became less dense and looser in structure. Although the strength would increase in the late stage, the overall strength of the system eventually decreased [27].

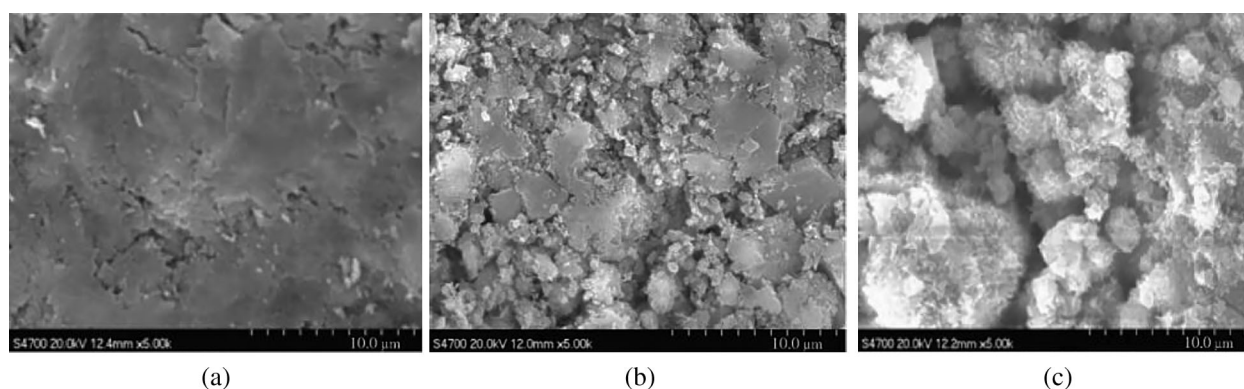


Figure 6: SEM photos of the hydration products (14h) (a) Cement paste (b) Tailings content 15% (c) Tailings content 45%

If copper tailings are applied to mass concrete, this defect could be made up by strengthening grinding and prolonging calcination, so as to enhance the activity of the materials. Further research is needed to fully remedy this defect.

For the cementitious materials slurry with 15%, 30% and 45% of copper tailings, hydration exothermic reaction rates are plotted in Fig. 7a. It can be seen that the low contents of active substances in copper tailings can extend hydration induction period. The larger the content is, the longer the second exothermic peak time will be [28], the overall hydration rate will also decline and the hydration time will be significantly prolonged, which is not suitable for the conventional structure engineering. However, copper tailings have a significant weakening effect on the early heat release rate and total heat release [29], which provides the possibility of application in mass concrete engineering.

In Fig. 7b, the content of copper tailings is 45%, the water-binder ratio of concrete is still 0.4. It can be seen from the figure that the high content of copper tailings makes the difference of peak value larger between the two curves, this shows that the admixture affects the hydration of cement. During the process of NG, the reaction resistance is relatively large, which results in the delay of the initial setting time, makes the hydration rate slower, delays the final setting time, and prolongs the acceleration period [30,31]; during the process of I, the hydration rate is faster, and the secondary hydration of the mineral admixture begins to play a leading role; in the process of D, the hydration rate is still faster, which makes the deceleration period longer.

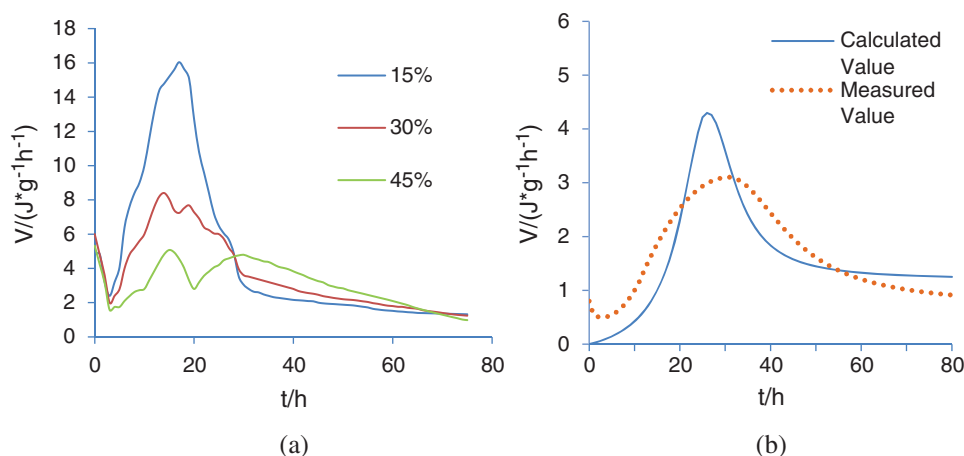


Figure 7: (a) Comparison with different contents (b) between calculated and measured value

5 Conclusions

Based on the experiment and numerical calculation, the findings of this study can be summarized as,

(1) This microscopic hydration model can accurately predict the hydration process of concrete taking cement and copper tailings as composite cementitious materials.

(2) Based on the improved microscopic hydration model, the hydration degree, hydration rate and other parameters are obtained, and then concrete macroscopic heat and moisture coupling diffusion model is established, which can predict the temperature and humidity distribution of early-age concrete.

(3) If no activator is added, the amount of copper tailings should not exceed 30%; The concrete with the larger mixing percentage of copper tailings can be attempted in mass concrete projects, which needs to be further investigated.

Funding Statement: This work was financially supported by Provincial Quality Engineering Project of Anhui Province of China [Grant Nos. 2019xfxm71 and 2020-6656].

Conflicts of Interest: The authors declare that they have no conflicts of interest to report regarding the present study.

References

1. Klemczak, B. (2011). Prediction of coupled heat and moisture transfer in early-age massive concrete structures. *Numerical Heat Transfer Part A: Applications*, 6(3), 212–233.
2. Saeki, T., Monteiro, P. J. (2005). A model to predict the amount of calcium hydroxide in concrete containing mineral admixtures. *Cement and Concrete Research*, 35(10), 1914–1921.
3. Tang, S. B., Tang, C. A. (2011). Numerical simulation research on humidity diffusion characteristics of cement-based composites at mesoscopic level. *Journal of Dalian University of Technology*, 15(6), 868–874.
4. Mu, R., Forth, J. P. (2009). Modelling shrinkage of concrete from moisture lost using moisture diffusion theory. *Magazine of Concrete Research*, 61(7), 491–497.
5. He, F. Y., Chen, Z. H. (2020). Relative humidity analysis of early-aged concrete base on temperature and humidity interaction. *Journal of Civil and Environmental Engineering*, 42(1), 108–115.
6. Krstulovic, R., Dabic, P. (2000). A conceptual model of the cement hydration process. *Cement and Concrete Research*, 30(5), 693–698.
7. Moon, H., Ramanathan, S., Suraneni, P. (2018). Revisiting the effect of slag in reducing heat of hydration in concrete in comparison to other supplementary cementitious materials. *Materials*, 11(10), 1847–1858.

8. Dang, H. F., Xie, Q. Q. (2019). Study on hydration characteristics of composite cementitious system based on Krstulovic-Dabic model. *Bulletin of the Chinese Ceramic Society*, 38(3), 722–728.
9. Sakata, K. A. (1983). Study on moisture diffusion in drying and drying shrinkage of concrete. *Cement and Concrete Research*, 13(2), 216–224.
10. Wang, Y. W. (2014). *Study of hydration mode of cement with mineral admixtures and its application*, (Master's Thesis). Hangzhou, China: Zhejiang University.
11. Lv, Q. H., Xiao, L. Z. (2020). Temperature effect of cement-based materials based on hydration kinetics model. *Journal of Wuhan Institute of Technology*, 42(4), 432–438.
12. Wang, P. M., Li, N., Xu, L. L. (2017). Hydration evolution and compressive strength of calcium sulphoaluminate cement constantly cured over the temperature range of 0 to 80°C. *Cement and Concrete Research*, 100, 203–213.
13. Thomas, B. S., Damare, A., Gupta, R. C. (2013). Strength and durability characteristics of copper tailing concrete. *Construction & Building Materials*, 48(11), 894–900.
14. Li, Q. L. (2018). *Mechanism effects of copper tailings in cement-based materials*, (Ph.D. Thesis). Wuhan University.
15. Li, B., Jin, N., Tian, Y. (2020). Numerical analysis and experimental study on heat-moisture-carbonation. *Journal of Building Materials*, 23(1), 145–150.
16. Gupta, T., Sachdeva, S. N. (2019). Laboratory investigation and modeling of concrete pavements containing steel slag. *Cement and Concrete Research*, 124(10), 172–182.
17. Zhang, J., Wang, J., Gao, Y. (2015). Moisture movement in early-age concrete under cement hydration and environmental drying. *Magazine of Concrete Research*, 68(78), 391–408.
18. Neffah, Z., Kahalerras, H., Fersadou, B. (2018). Heat and mass transfer of a non-newtonian fluid flow in an anisotropic porous channel with chemical surface reaction. *Fluid Dynamics & Materials Processing*, 14(1), 39–56.
19. Wong, S. F., Wee, T. H., Swaddiwudhipong, S., Lee, S. L. (2001). Study of water movement in concrete. *Magazine of Concrete Research*, 53(3), 205–220.
20. Kang, S. T., Kim, J. S., Lee, Y., Park, Y. D., Kim, J. K. (2012). Moisture diffusivity of early age concrete considering temperature and porosity. *Ksce Journal of Civil Engineering*, 161, 179–188.
21. Ye, X. D. (2017). *Study on the micromechanism and mechanical properties of copper tailing powder concrete*, (Ph.D. Thesis). Yunnan, China: Yunnan University.
22. Wang, Y., Hu, X. Y. (2018). Coupled heat and moisture transfer features of typical external thermal insulation systems. *International Journal of Heat and Technology*, 36(4), 1362–1366.
23. Naraigh, O. L., Jansen, D. R. (2020). Linear and nonlinear stability analysis in microfluidic systems. *Fluid Dynamics & Materials Processing*, 16(2), 383–410.
24. Hou, D. W. (2010). *Integrative studies on autogenous and drying shrinkage of concrete and related issues*, (Ph.D. Thesis). Beijing, China: Tsinghua University.
25. Reda, R. (2019). Constrained groove pressing (CGP): Die Design, material processing and mechanical characterization. *Fluid Dynamics & Materials Processing*, 15(3), 171–185.
26. Esmaeili, J., Aslani, H. (2019). Use of copper mine tailing in concrete: Strength characteristics and durability performance. *Journal of Material Cycles and Waste Management*, 21(1), 729–741.
27. Kundu, S., Aggarwal, A., Mazumdar, S., Dutt, K. B. (2016). Stabilization characteristics of copper mine tailings through its utilization as a partial substitute for cement in concrete: Preliminary investigations. *Environmental Earth Sciences*, 75(3), 1–9.
28. Scrivener, K. L., Juilland, P., Monteiro, P. J. M. (2015). Advances in understanding hydration of portland cement. *Cement & Concrete Research*, 78(12), 38–56.
29. Thomas, B. S., Damare, A., Gupta, R. C. (2013). Strength and durability characteristics of copper tailing concrete. *Construction & Building Materials*, 48(11), 894–900.
30. Esmaeili, J., Aslani, H. (2019). Use of copper mine tailing in concrete: Strength characteristics and durability performance. *Journal of Material Cycles and Waste Management*, 21(3), 729–741.
31. Dang, H. F., Long, G. C., Ma, C. (2019). Effect of temperature on hydration kinetics of cement system with mineral admixtures. *Journal of Railway Science and Engineering*, 16(4), 907–914.